

# Airtightness of roof cavities

Stephan Rupp, Manfred Plagmann and Ian Cox-Smith





Funded from the  
Building Research Levy



1222 Moonshine Rd, RD1, Porirua 5381  
Private Bag 50 908, Porirua 5240  
New Zealand  
[branz.nz](http://branz.nz)

© BRANZ 2018  
ISSN: 1179-6197

## Acknowledgements

This work was funded by the Building Research Levy under projects DR0803 Interstitial Moisture in Roof Cavities and MR0002 Monitoring Conditions and Air Flows in Roofs. The support is greatly appreciated.



# Airtightness of roof cavities

## BRANZ Study Report SR401

### Authors

Stephan Rupp, Manfred Plagmann and Ian Cox-Smith

### Reference

Rupp, S., Plagmann, M. & Cox-Smith, I. (2018). *Airtightness of roof cavities*. BRANZ Study Report SR401. Judgeford, New Zealand: BRANZ Ltd.

### Abstract

We have introduced and trialled a measurement procedure to estimate the airtightness of residential roof spaces. By using a dual fan approach, it is possible to distinguish between the leakage through the roof envelope and the air permeability of the ceiling. Using this method, an effective leakage area for three residential dwellings with and without mould growth in the attic space is calculated and compared to international standards.

In addition, the air permeability of common New Zealand ceilings and ceiling penetrations has been characterised in a specially designed test facility. The datasets are given in a tabular form and can be used in numerical simulations.

### Keywords

Airtightness, roof cavities, ventilation.

## Contents

<b>1. INTRODUCTION .....</b>	<b>1</b>
<b>2. AIR PERMEABILITY MEASUREMENTS OF CEILINGS AND FIXTURES .....</b>	<b>2</b>
2.1 Experimental – ceiling tests.....	2
2.2 Experimental – ceiling fixtures.....	4
2.3 Results .....	5
2.3.1 Pressure difference across the ceiling of a single-storey residential building .....	5
2.3.2 Air permeability of ceilings.....	6
2.3.3 Air permeability of ceiling fixtures .....	8
<b>3. AIRTIGHTNESS TESTS OF ROOF CAVITIES .....</b>	<b>9</b>
3.1 Experimental set-up for roof cavity airtightness measurements .....	9
3.2 Characterisation of the test buildings .....	12
3.2.1 BRANZ ventilation test building .....	12
3.2.2 Residential building, Titirangi, Auckland.....	14
3.2.3 Residential building, Papakura, Auckland .....	17
3.2.4 Summary and discussion .....	19
3.2.5 Example: calculation of required roof ventilation.....	20
<b>4. CONCLUSIONS AND OUTLOOK.....</b>	<b>22</b>
<b>REFERENCES .....</b>	<b>23</b>
<b>APPENDIX A: FAN CALIBRATION .....</b>	<b>24</b>

## Figures

Figure 1. Test facility for air permeability of ceilings. Left: sketch of the test room with airtight walls and timber rafters for convenient installation of different ceiling types. Right: layout of the test facility within the roof ventilation test building...2	2
Figure 2. Left: front wall and entry door of the ceiling test facility. The fan used to pressurise the room is attached to a laminar-flow element (cylindrical device in the background), which measures the volumetric airflow into the room. Right: view from the inside with no ceiling installed .....	3
Figure 3. Set-up to characterise small device for its airflow characteristics. ....4	4
Figure 4. Measured pressure difference across a residential ceiling (blue) and wind speed at 10 m height. ....5	5
Figure 5. Correlation between pressure difference and wind speed.....6	6
Figure 6. Statistical box plot of the pressure data $\Delta p$ from Figure 4. 25% and 75% quartiles (yellow box), median (black line), 5% and 95% whiskers and outliers (points) are plotted. ....6	6
Figure 7. Dual fan method to characterise the airtightness of a roof cavity.....10	10
Figure 8. Dual fan set-up to characterise the airtightness of a roof cavity. Left: no pressure difference across the ceiling lining as both spaces are pressurised to the same value. Right: with fan 1 switched off, resulting in air flowing down. .10	10
Figure 9. Airflow data with the ceiling neutralised (blue) and contributing to the airflow (orange) – data from the Titirangi residence. ....11	11
Figure 10. BRANZ Ventilation test building in Judgeford.....12	12

Figure 11. Airflow versus pressure for the ventilation test building – ceiling balanced to 0 Pa. The curve fit using Equation 1 is given. Right: leakage paths visualised by a smoke generator in the attic.....	13
Figure 12. Top: calculated air exchange rates for the attic space based on a tracer gas measurement. Climatic conditions and gas concentrations are also given.....	14
Figure 13. Examples of mould growth on roofing paper and timber. ....	15
Figure 14. Downlight as viewed from the attic space. The large opening around the main body is visible.....	15
Figure 15. Relative humidity in the main bedroom, attic space, bathroom and kitchen of the Titirangi dwelling. ....	16
Figure 16. Statistical distribution of relative humidity for the Titirangi dwelling. The boundaries of the coloured boxes indicate the 25% and 75% quartile, the line represents the median, while the whiskers give the maximum and minimum values. ....	17
Figure 17. Measurement set-up with dual fan blower door (left) and ducting into the roof cavity (right). ....	18
Figure 18. Airflow results for the Papakura dwelling. The measured data points are fitted using Equation 1. ....	18
Figure 19. Statistical distribution of relative humidity for the Papakura dwelling. The boundaries of the coloured boxes indicate the 25% and 75% quartile, the line represents the median, while the whiskers give the maximum and minimum values. ....	19
Figure 20. Sketch of airflows for the mass balance calculation.....	20
Figure 21. Restrictor plate configurations for the Retrotec fans. ....	24

## Tables

Table 1. Air permeability data for ceilings.....	7
Table 2. Air permeability data for ceiling fixtures.....	8
Table 3. Ventilation parameters for the three studied dwellings.....	19
Table 4. Ducting error results. ....	24



## 1. Introduction

Residential buildings in New Zealand have become increasingly airtight over the last decades (McNeil et al., 2012; Overton, 2018). The reason for this lies in more modern building materials and components as well as improved construction practices.

Aluminium window joinery in comparison to draughty wooden windows and concrete slabs in contrast to tongue and groove floorboards are two examples. An increased level of airtightness has the obvious energy benefit of making it easier to heat the building, as warm air cannot readily escape through gaps and openings in the envelope. However, improved airtightness also means fewer natural exchanges of the indoor air. If the building is not adequately ventilated, moisture and pollutants can build up over time to a level where problems might occur.

There have been efforts to characterise the airtightness of residential living spaces, and good quality data indicating a clear trend to more sealed buildings is available. However, the situation is less clear for roof cavities. There are two main reasons for the lack of airtightness data of roof cavities:

- There has not been much interest in this data. While airtightness testing of the living space has gained some popularity in order to evaluate a building's energy performance, the roof cavity is less relevant from this point of view.
- Typical equipment used to characterise the airtightness of a building – a blower door set-up – is typically not powerful enough to cope with the often much leakier roof cavity.

Recently, the focus has shifted to the attic space as moisture related problems have been noted in newly built residential houses (Rupp & Plagmann, 2016; Essah, 2012). The question arises: how can moisture accumulate to a level where it causes mould growth on structural timber and roofing paper? The airtightness of the attic is relevant since it governs the air-exchange rate (wind and stack pressure driven) and thus the removal of potential excess moisture (Plagmann, 2016). The air permeability of the ceiling level is of interest since it determines how easily warm, moist air from the living space can move up into the roof space and possibly accumulate there.

In this study, we have made a start to address these relevant issues:

- In section 2, we characterise a number of typical New Zealand ceiling linings and fixtures for their air permeability properties. The results are presented in table form, with some examples given to illustrate their relevance.
- In section 3, we describe a measurement set-up developed that is capable of deriving approximate airtightness data and an effective air leakage area for a range of residential roof spaces. This set-up was trialled on buildings with and without moisture problems in the attic. Comparisons between our blower door type measurement with tracer gas type measurements are given.

## 2. Air permeability measurements of ceilings and fixtures

Many residential buildings in New Zealand have a cold roof design (Rupp, 2018). Thermal insulation is installed above the ceiling lining, leaving a cavity underneath the cladding that is close to the ambient temperature modulated only by the achieved R-value. While heat and water can move from the living spaces into the roof cavity by conduction and diffusion, the dominant transport mechanism is convection – the movement of air through cracks, gaps and opening (Essah, 2012). Depending on the ceiling type, detailing, quality of the installation and the number of penetrations such as downlights and roof access hatches, the ceiling can be an effective air barrier.

In this section, a range of common ceiling types and fixtures are described in terms of their air permeabilities. The experimental details and underlying physical principles are briefly discussed. The results section 2.3 includes measurements of actually encountered pressure differences across a residential ceiling due to wind action and stack effect.

### 2.1 Experimental – ceiling tests

In order to evaluate the air permeability of different, common ceiling linings a special test facility (Figure 1) was designed and constructed within one of our experimental buildings on the BRANZ site in Judgeford. Efforts were made to seal the wall linings and the entry door of the 38.1 m<sup>2</sup> room within a room as best as possible. The area is deemed large enough to account for variations in material and workmanship. A design of timber ceiling rafters was chosen to allow for an easy and flexible installation of the different ceiling types to be tested.

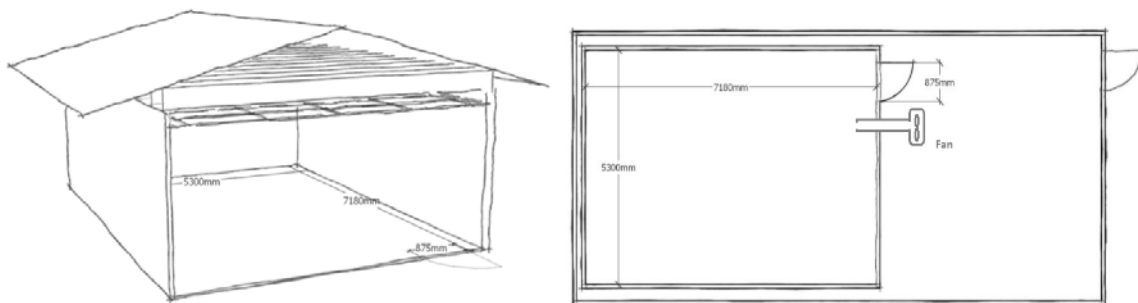


**Figure 1. Test facility for air permeability of ceilings. Left: sketch of the test room with airtight walls and timber rafters for convenient installation of different ceiling types. Right: layout of the test facility within the roof ventilation test building.**

The airflow rate as a function of the pressure difference across the material is described by the leakage function (ASHRAE, 2009, Chapter 16, Equation 40):

$$Q = c \cdot \Delta p^n \quad Eq\ 1$$

where

$Q$  volumetric airflow rate [m<sup>3</sup>/s]

$c$  flow coefficient characteristic for the ceiling or fixture [m<sup>3</sup> / (s Pa<sup>n</sup>)]



$\Delta p$  pressure difference across the ceiling [Pa]

$n$  pressure exponent, describing the nature of the flow (going from a factor of 0.5 indicating turbulent to 1 for a laminar flow) [dimensionless]

To obtain the characteristic material properties  $c$  and  $n$  for a specific ceiling, the following test procedure is performed. Using a fan, air is forced into the room at a constant rate (parameter  $Q$  in the above formula). This volumetric airflow measurement is achieved using a Laminar Flow Element (LFE)<sup>1</sup> (Figure 2).



**Figure 2. Left:** front wall and entry door of the ceiling test facility. The fan used to pressurise the room is attached to a laminar-flow element (cylindrical device in the background), which measures the volumetric airflow into the room. **Right:** view from the inside with no ceiling installed

At the same time, the pressure difference  $\Delta p$  across the ceiling is recorded for this airflow. Doing this for a number of different parameter pairs  $Q$  and  $\Delta p$ , we obtain a dataset that can be fitted using Equation 1 with  $c$  and  $n$  being the fit parameters. While the parameter  $c$  describes the 'leakiness' of the material, the latter fit parameter  $n$  characterises the nature of the flow.

The airflow rate is sometimes converted into an effective air leakage area (ASHRAE, 2009, Chapter 16, Equation 41):

$$A_L = \frac{10\,000 Q}{C_D} \sqrt{\frac{\rho}{2 \Delta p_r}} \quad \text{Eq 2}$$

<sup>1</sup> Meriam Model Z50MR2-6.

where

- $A_L$  effective air leakage area [ $\text{cm}^2$ ]
- $Q$  volumetric airflow rate [ $\text{m}^3/\text{s}$ ]
- $\rho$  air density [ $\text{kg}/\text{m}^3$ ]
- $\Delta p_r$  reference pressure difference [Pa]
- $C_D$  discharge coefficient [dimensionless]

Experiments are performed pressurising the room (rather than depressurising) to reflect the most common situation in buildings. Usually wind action across the envelope of a building will result in a slight negative pressure of the attic space with respect to the living quarters. Section 2.3.1 summarises actual pressure data across a residential ceiling recorded in the BRANZ ventilation test building over the period of a week. Results from this experiment and the need to obtain good datasets for fitting purposes meant the maximum pressure across the tested ceilings was chosen to be between 15 and 20 Pascals. The volumetric airflow per time interval  $Q$  and the coefficient  $c$  can be normalised to reflect sensible units for the tested product. For example, a homogeneous ceiling material would best be described normalised to an area in cubic metres per second per area of ceiling [ $\text{m}^3/\text{s}/\text{m}^2$ ]. On the other hand, linear elements such as scotia trimmings or expansion control joints are best described in terms of leakage per unit length [ $\text{m}^3/\text{s}/\text{m}$ ].

## 2.2 Experimental – ceiling fixtures

The characterisation of ceiling penetrations such as light fittings and roof access hatches works in a similar way but on a smaller scale. An airtight enclosure is used to house the device under test (Figure 3). The measurement procedure is otherwise the same as with the ceilings.



**Figure 3. Set-up to characterise small device for its airflow characteristics.**



## 2.3 Results

### 2.3.1 Pressure difference across the ceiling of a single-storey residential building

Figure 4 shows differential pressure measurements across a plasterboard ceiling on the single-storey BRANZ ventilation test building. Wind speed in close proximity to the test building at a height of 10 m is also plotted. The data was acquired over a period of 5 days with wind speeds close to zero and up to 6 m/s (~22 km/h). Windows and doors were kept shut during the experiment. While the sampling interval was 1 minute, the data displayed in Figure 4 has been smoothed by a moving average routine. The recorded pressure differences are exclusively such that the roof cavity has a negative pressure in comparison to the living space. Thus, the air transport will be predominantly in the direction from the living space to the attic space (Roppel, Norris & Lawton, 2013).

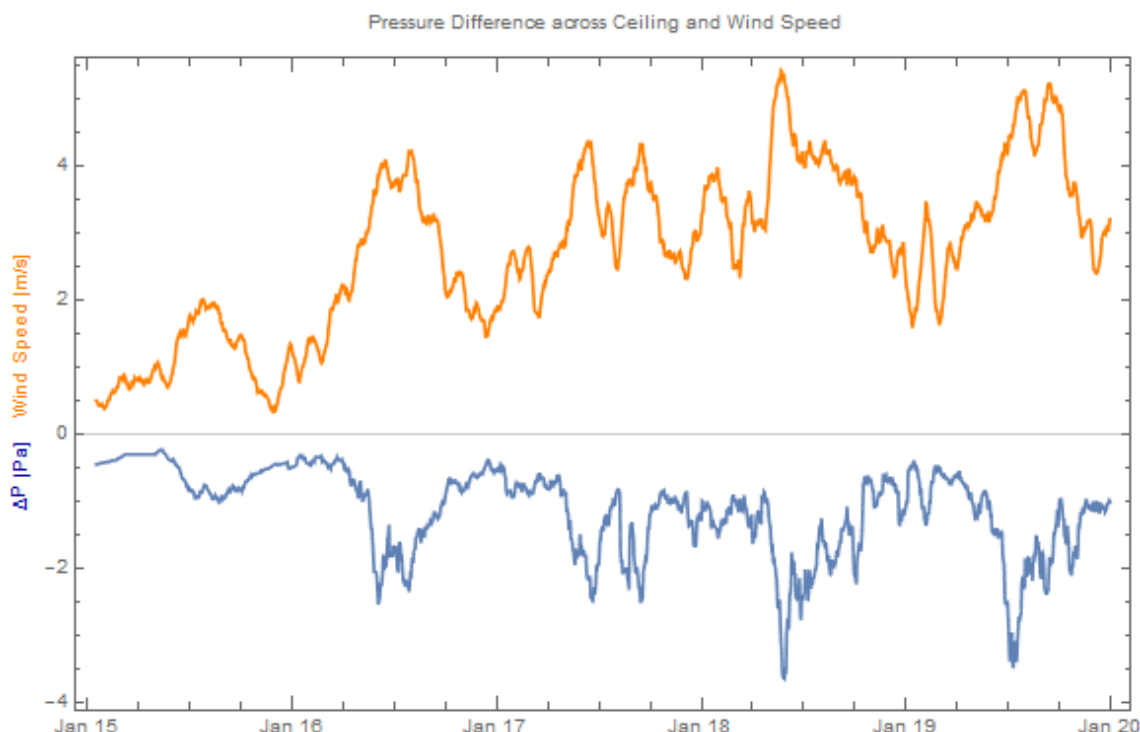


**Figure 4. Measured pressure difference across a residential ceiling (blue) and wind speed at 10 m height.**

A reasonably pronounced correlation of pressure difference  $\Delta p$  to the wind velocity can be seen (see also Figure 5). For the encountered wind conditions during our measurement period, the recorded pressures lie between 0.5 and 4 Pascals. The wind direction and internal temperature differences will play a role in the pressure gradient across the ceiling but have been neglected here.

During our measurement campaign, the wind direction was mostly from the north with little variation. The temperature in the attic was around 40°C during the day, dropping to around 18°C at night. In the living space these figures were 30°C and 20°C during day and night respectively. Wind action seems to be the dominant driver for the pressure difference across the ceiling.

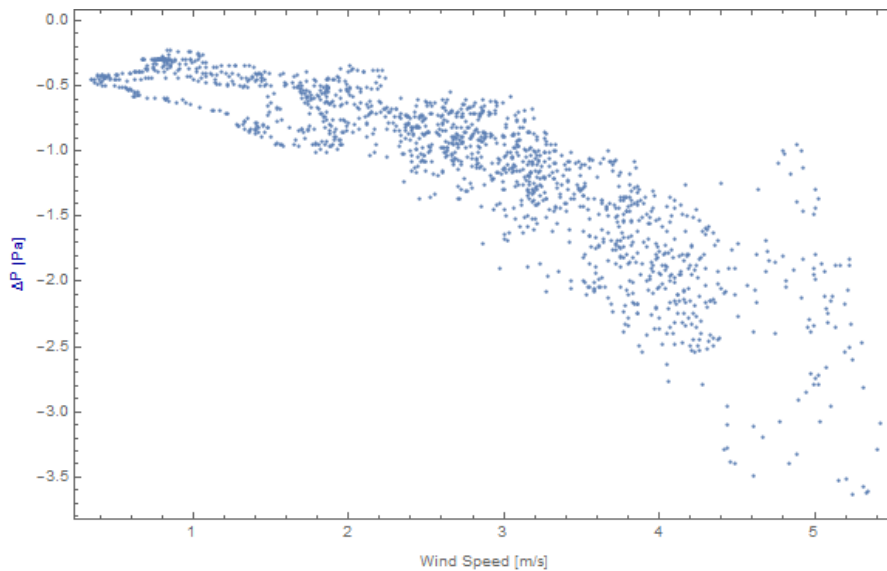


**Figure 5. Correlation between pressure difference and wind speed.**

Figure 6 displays the measured pressure data as a box whisker plot indicating the key statistical parameters.

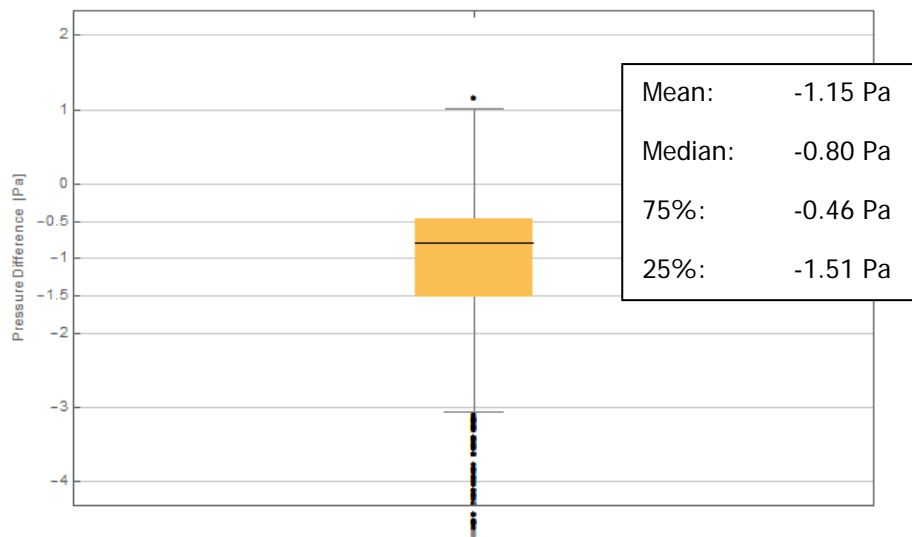


**Figure 6. Statistical box plot of the pressure data  $\Delta p$  from Figure 4. 25% and 75% quartiles (yellow box), median (black line), 5% and 95% whiskers and outliers (points) are plotted.**

For this experiment with average wind speeds of 2.7 m/s (~10 km/h), approximately half of all measured pressure values fall with an interval between  $-0.5 > \Delta p > -1.5$  Pascals. The mean value is  $\Delta p_{\text{mean}} = -1.2$  Pascals. This is also the pressure that is used in the following sample calculations.

### 2.3.2 Air permeability of ceilings

Air permeability measurements of a variety of residential and commercial ceiling types are summarised in Table 1. Five different ceiling types were installed. Suspended acoustic ceiling tiles are a common choice in commercial buildings and schools around New Zealand. They are easy to install and allow convenient access to ducting, cables and so on. A plywood ceiling using 12 mm thick panels was installed in two different

configurations – either with a tight fit or with a 5 mm gap between the panels. No glue was used with any of the installed components.

**Table 1. Air permeability data for ceilings.**

	Ceiling Type	Image	Air Flow Formula	Flow Coefficient $c$	Exponent $n$
Airflow per area of installed product	Acoustic Ceiling Tiles - suspended 900x1200mm each		$Q [l / (s m^2)] = c \Delta P^n$	<b>0.56</b>	<b>0.89</b>
	T&G timber ceiling 80mm width			<b>0.07</b>	<b>0.77</b>
	Plywood tight fit 1200x2400x12mm each			<b>0.01</b>	<b>0.81</b>
	Plywood 5 mm gap 1200x2400x12mm each			<b>0.05</b>	<b>0.71</b>
Airflow per length of installed product	Scotia on Plasterboard		$Q [l / (s m)] = c \Delta P^n$	<b>0.02</b>	<b>0.84</b>
	Plasterboard Control Joint			<b>0.02</b>	<b>0.88</b>

Depending on the relevant dimension of the product installed, the results are normalised to an area or a linear length. For instance, the air leakage characteristic of acoustic ceiling tiles will be cited per area of installed product, while the leakage rate of timber scotia installed over a plasterboard corner will be normalised to a linear length.

Taking the acoustic tiles as an example, a 10 m<sup>2</sup> ceiling area with a constant pressure difference of  $\Delta p = 1.2$  Pascals across it would result in an airflow of  $Q = 6.6$  litres/second. The ceiling tiles are by far the leakiest type of ceiling in this measurement series, followed by the tongue and groove (T&G) timber system. BRANZ recommends an air barrier be installed behind T&G ceilings on skillion type roof designs to restrict the amount of (possibly moist) air entering the roof cavity (BRANZ, 2017). Due to the nature of suspended acoustic tiles, an air barrier is not easy to install, which is contributing to moisture-related problems in some New Zealand schools (BRANZ, 2014). Plywood as a ceiling lining is less leaky than the T&G option.

However, the air permeability can vary significantly depending on the installation. Leaving a 5 mm gap between sheets has increased the flow coefficient by roughly a factor of 5.

A standard plasterboard ceiling was installed and measured in this experiment but is not listed in the table. A fully square-stopped plasterboard lining is assumed to be a near-perfect air barrier and served here to evaluate the background losses of our experimental test enclosure. Installing timber scotias instead of the square stopping introduces an air leakage path, which is given in the table per unit length. A plasterboard control joint has similar leakage properties to the scotia.

### 2.3.3 Air permeability of ceiling fixtures

An otherwise airtight ceiling can easily be downgraded by penetrations for lighting, access hatches and other services. Downlights have become very popular, and it is not uncommon to find dozens of such lights installed in a residential building. Old-style incandescent or halogen-type lights require space around them to dissipate heat and represent a direct channel from the living space into the roof cavity.

In this study, only a limited number of fixtures could be characterised. Air leakage data for a range of representative styles is given in Table 2.

**Table 2. Air permeability data for ceiling fixtures.**

	Element	Image	Air Flow Formula	Flow Coefficient C	Exponent n
Airflow rate per unit installed	Classic Roof Space Access Hatch		$Q [l / s] = c \Delta P^n$	<b>0.87</b>	<b>0.58</b>
	Downlight, incandescent old style			<b>1.60</b>	<b>0.46</b>
	Downlight, incandescent new style			<b>0.40</b>	<b>0.59</b>
	Downlight, Halogen bulb			<b>0.06</b>	<b>0.69</b>
	Downlight, LED tight fit			<b>0.02</b>	<b>0.71</b>

It is likely that, within each category, there will be significant difference, depending on the design details. However, it is apparent that the new generation of tightly fitted LED downlights, which do not require any open space for ventilation, offer significantly improved performance from an air permeability view. Some LED downlights are fitted with a rubber gasket, which essentially offers a sealed system.

Similarly, although not tested yet in this report, more airtight and insulated roof access hatches are commercially available.



### 3. Airtightness tests of roof cavities

As described in the introduction, an airtight building envelope is desirable from an energy point of view. Heat losses in cold climates are reduced by minimising convective transport processes. However, it also means that moisture from internal sources can accumulate if no adequate ventilation is provided. Since warm, moist air rises and wind action across the envelope is usually driving air from the living areas into the attic, an airtight roof cavity can be problematic. Passive roof space ventilation openings are mandatory or recommended in some countries like the USA or Canada. The size of such ventilation elements is often described as a ratio between the net free opening of the vent elements to the ceiling insulated area. While ratios ranging from 1:150 to 1:600 can be found, 1:300 seems to be a frequently specified fraction (Roppel et al., 2013; Lstiburek, 2004). Currently, there is no requirement to ventilate roof cavities in New Zealand.<sup>2</sup> The ratio of 1:300 is therefore used in this report as a comparison.

#### 3.1 Experimental set-up for roof cavity airtightness measurements

The airtightness of the roof cavity is determined by using an adapted blower door type approach as described below.

In a typical blower door measurement, the airtightness of a building is evaluated by pressurising (or depressurising) the entire living space over a range of indoor/outdoor static pressure differences. The airflow into or out of the building at any such given pressure difference is recorded. Commercial testing devices typically consist of a door mount with a mechanical fan that can be operated at variable speeds to achieve the desired airflow rates. The apparatus, measurement procedure and expression of results are described by AS/NZS ISO 9972:2015 *Thermal performance of buildings – Determination of air permeability of buildings – Fan pressurization method*.

A parameter that is often used to evaluate the airtightness of a building is the n50 value. The air leakage rate at an applied pressure of 50 Pascals is converted to an air exchange per hour value (ach) by normalising it with the internal volume of the building. Typical n50 values for the living spaces of newly built residential homes are around 3–5 ach.

It is important to note that the primary purpose of these measurements is to derive an effective air leakage area as derived by Equation 2. The obtained air exchange figures are for evaluative and comparative use only. Under normal conditions, the pressure differences between the inside and the outside are substantially lower than the reference pressure of 50 Pascals, yielding much smaller actual ventilation rates.

Sometimes, the n50 value is divided by a factor of 20 to give an approximate value for the infiltration rate under normal climatic conditions (Liddament, 1986). However, this value is dependent on many factors and can be between 20–50 and thus is only a rough estimate of the expected long-term average. For a more realistic air exchange value, a tracer gas method is preferable (Sherman, 1990).

---

<sup>2</sup> Some regional councils require roof ventilation for high-risk buildings.



Figure 7 shows the dual blower door fan<sup>3</sup> set-up in the BRANZ ventilation test building, which has been developed to characterise the airtightness of residential roof cavities. Fan 1 is used to pressurise the living space, while fan 2 is channelling outside air via ducting into the roof space.

This set-up is chosen so that the leakage area of only the roof envelope can be determined. If both the living space and the roof space are pressurised to the same value, there will be no airflow across the ceiling lining.



**Figure 7. Dual fan method to characterise the airtightness of a roof cavity.**

This situation is depicted on the left in Figure 8, where both the roof cavity and the living space are pressurised to 40 Pascals. Windows and doors are shut for this measurement mode.

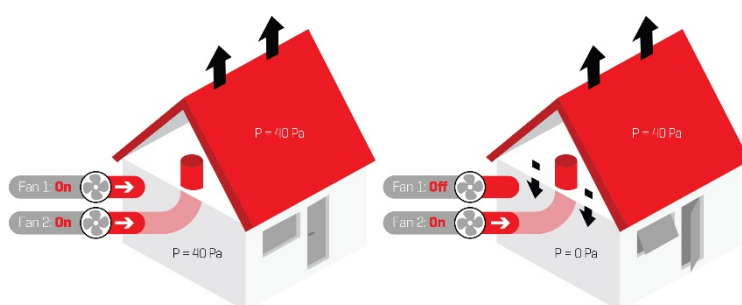


**Figure 8. Dual fan set-up to characterise the airtightness of a roof cavity. Left: no pressure difference across the ceiling lining as both spaces are pressurised to the same value. Right: with fan 1 switched off, resulting in air flowing down.**

<sup>3</sup> Retrotec Ltd Series 5000 and 6000 fans and dual fan door cloth.



With fan 1 turned off, the ceiling lining will be exposed to a pressure drop across it, and air will be forced downstairs through any cracks and openings. Windows and doors should be opened to ensure that the building is at ambient pressure.

Figure 9 shows these two measurement configurations performed on a residential building in Titirangi, Auckland. The measured data (dots) is fitted using Equation 1, yielding a good result. While the blue curve represents the airflow through and around the roof cladding only, the difference between the two curves can be attributed to an additional airflow through the ceiling lining and penetrations.

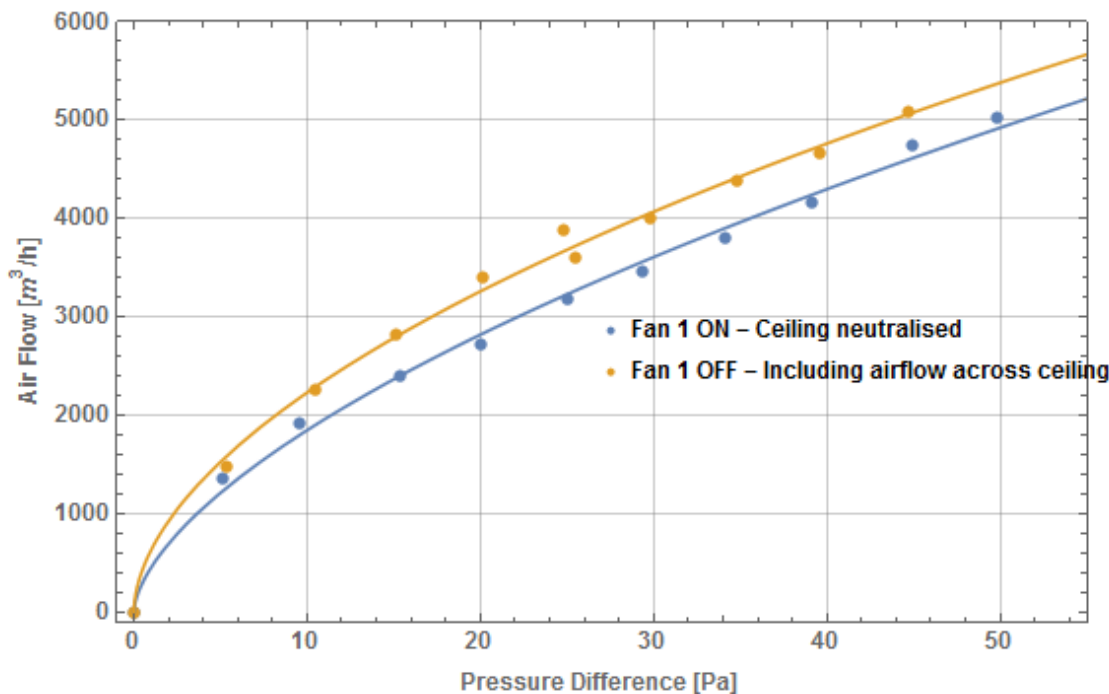


**Figure 9. Airflow data with the ceiling neutralised (blue) and contributing to the airflow (orange) – data from the Titirangi residence.**

In this case, the roof cavity was reasonably tight, and for the balanced measurement, a pressure difference of close to 50 Pa was achieved. While this is a desired reference value for a standard blower door test on residential buildings, it is not always possible to reach this pressure in roof cavities due to their leaky nature. The analysis in section 3.2 is performed based on 40 Pascals.

It was found that, under certain operating conditions, the measured airflow rate suffers from systematic errors when ducting is attached to the fan. A detailed description is given in Appendix A.

Essentially, the airflow rate through the fan is obtained by a calibration of the measured pressure difference across the nacelle. The fan opening and thus the airflow rate can be adjusted by a number of restrictor plates. It was found that removing all restrictor plates in combination with the ducting leads to significant errors. This operating mode was avoided for the experiments in this study.



## 3.2 Characterisation of the test buildings

### 3.2.1 BRANZ ventilation test building

The method using a dual fan set-up was trialled on the BRANZ ventilation test building (Figure 10). In addition to the pressurisation experiments, a tracer gas approach was trialled to determine actual infiltration rates of the roof cavity under normal climatic conditions.



**Figure 10. BRANZ Ventilation test building in Judgeford.**

The gable-type construction has a standard corrugated iron cladding on building paper on mesh. The insulated ceiling area is approximately  $90 \text{ m}^2$ , yielding a roof cavity volume of around  $49 \text{ m}^3$ . No passive roof ventilation elements are installed in the building. The dwelling does not show any signs of mould in the roof space. While it is not inhabited and consequently does not have normal moisture sources, the building is frequently adjusted to high internal moisture levels for scientific purposes. The ceiling lining is standard plasterboard with square stopping. A number of artificial, controllable ventilation openings can provide an air exchange path from the living space to the roof cavity. For this experiment, these were shut.

Figure 7 shows the experimental set-up of the dual blower door fans in the BRANZ test building. The maximum pressure the system could build up in the attic space, with the ceiling balance close to zero pressure, was  $40 \text{ Pa}$  (Figure 11). At this attained pressure, the loss through the roof cladding was approximately  $5,930 \text{ m}^3/\text{h}$ . Fitting the data to Equation 1, we can estimate the airflow rate at  $P = 50 \text{ Pa}$  to be  $Q = 6,785 \text{ m}^3/\text{h}$ . Using the volume, this translates to an air exchange of  $n_{50} = 137 \text{ ach}$ . As mentioned above, these ventilation rates are not attained under normal conditions and are useful for comparisons only.

The results from our blower door measurements for all three buildings investigated in this study and the calculation and comparison of an effective air leakage area are given in section 3.2.4.

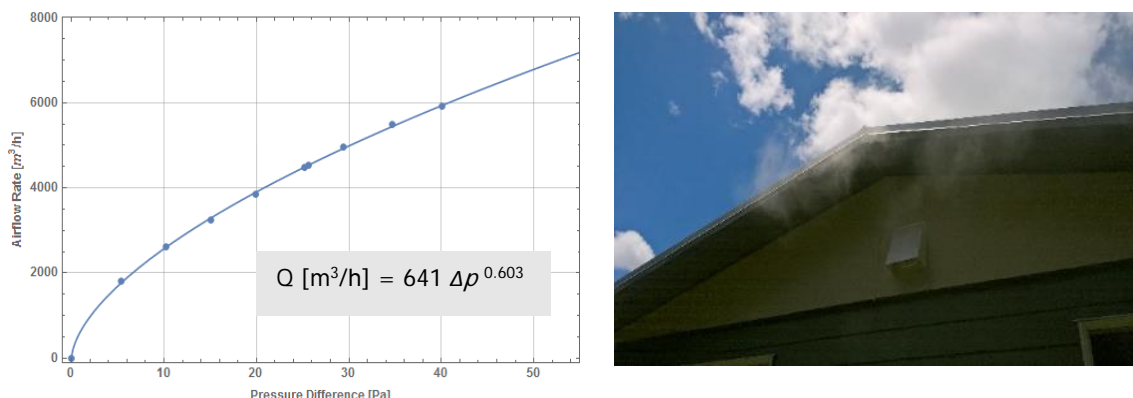


**Figure 11. Airflow versus pressure for the ventilation test building – ceiling balanced to 0 Pa. The curve fit using Equation 1 is given. Right: leakage paths visualised by a smoke generator in the attic.**

The air leakage through the roof envelope can be visualised using a smoke generator.<sup>4</sup> The battery-operated device was placed in the roof cavity, with a moderate pressure applied to the attic space. The main leakage paths were around the front and rear eaves, with lesser amounts coming from the soffit. No smoke could be detected exiting through the ridge cap from the overlap between iron sheets. These channels seem to be effectively blocked by the roofing underlay, at least for this crude visualisation method using smoke.

In addition to the blower door type characterisation of the roof cavity, a tracer gas experiment was also conducted. While pressurisation experiments with a blower door set-up can be used to compare individual buildings and determine effective leakage areas, the tracer gas method yields realistic air exchange rates under normal climatic conditions.

The attic space of the building was dosed with 1% SF<sub>6</sub> in N<sub>2</sub> at a constant rate of 40 ml/min for a period of 9 days. The sampling of the gas was performed in the attic space as well as outside the building every 5 minutes. The wind velocity was recorded at 10 metres above ground in close proximity to the dwelling. The measured gas concentration is used to calculate an infiltration rate (Sherman, 1990). Using the roof cavity volume, the latter can be expressed as air exchanges per hour (ach).

The calculated air exchange rate, measured gas concentrations as well as wind velocity and temperatures are given in Figure 12. The inverse correlation between gas concentration in the attic space and wind speed is as expected. Wind action is causing infiltration of outside air into the roof cavity, thus dilution of the tracer gas concentration.

The average air exchange rate for the roof cavity and this 9-day period was approximately 2.7 ach.<sup>5</sup> The 25% and 75% quartiles are 1.3 ach and 3.7 ach respectively.

<sup>4</sup> Retrotec.com

<sup>5</sup> Using a rule of thumb that relates an *n*50 blower door type measurement to an infiltration rate (see section 3.1), an air exchange rate of 137 ach/20 = 6.9 is obtained, showing the limitations of this approximation.

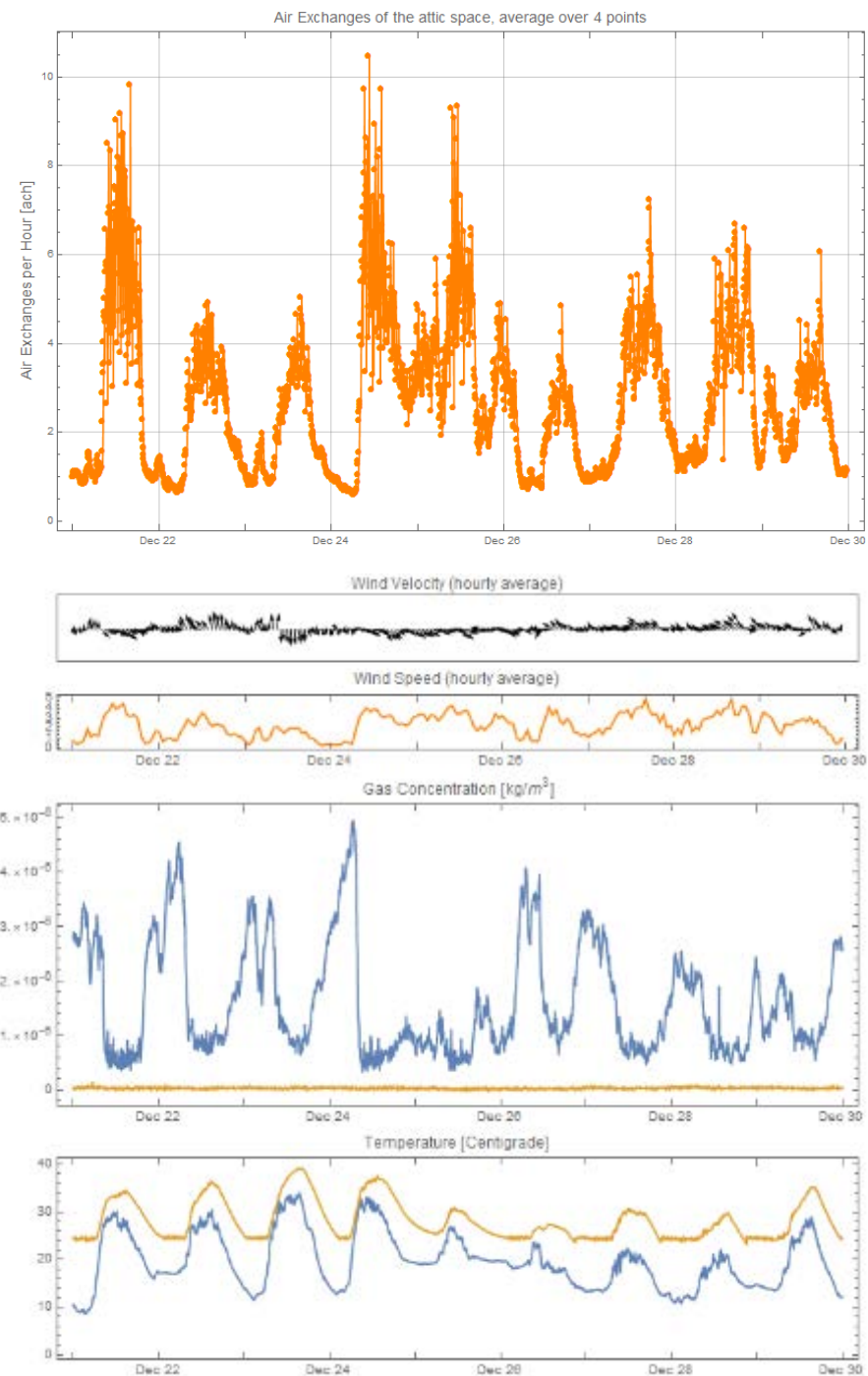


**Figure 12. Top:** calculated air exchange rates for the attic space based on a tracer gas measurement. Climatic conditions and gas concentrations are also given.

### 3.2.2 Residential building, Titirangi, Auckland

This 2-storey residential building in close proximity to the sea showed signs of extensive mould growth on the roofing paper as well as on the structural timber (Figure 13). The hilly surroundings are covered in tall vegetation shading the house, especially in the morning. The northern half of the building has a gable-type roof construction with a 75 m<sup>2</sup> area of insulated ceiling area. The front part of the building is covered by a skillion-type roof construction which is decoupled from the main roof cavity. The skillion part of the roof is not accessible and was not part of these measurements.



**Figure 13. Examples of mould growth on roofing paper and timber.**

The ceiling is lined with square-stopped plasterboard, which ordinarily would represent a good air barrier. However, 22 downlights installed through the top level provide an easy path for moisture from the living space into the attic. Although, the lights are of LED-type, the design is such that a gap exists between the main part and the mounting bracket (Figure 14). The individual light fitting could not be characterised as one of the elements in Table 2. Given the size of the opening, however, it is anticipated that the flow characteristic is in the same category as the very loose incandescent, old-style light fitting.



**Figure 14. Downlight as viewed from the attic space. The large opening around the main body is visible.**

Figure 9 shows the results for the blower door pressurisation measurements for this Titirangi property. The orange curve represents the data including an airflow back through the ceiling into the living space. Using fan 1, the ceiling flow has been neutralised to a negligible pressure drop represented by the blue dataset. The data shows some scatter due to the wind conditions during the experiment.

At 40 Pascals, the roof envelope alone exhibits an airflow of  $4,301 \text{ m}^3/\text{h}$  ( $n_{50}: 4,926 \text{ m}^3/\text{h}$ ) translating to an air exchange rate of 73 ach ( $n_{50}: 83 \text{ ach}$ ). Using Equation 2, an effective leakage area can be calculated (Table 3). Using the insulated ceiling area, a comparison can be made to the 1:300 roof ventilation area.



In this case, the ventilation opening to ceiling area ratio is 59% and would not be considered to meet the building code in some countries.

The flow across the ceiling only can be estimated by subtracting the two curves in Figure 9 for a given pressure level. Assuming a pressure difference<sup>6</sup> of 1.2 Pascals, the airflow across the ceiling alone is calculated to be approximately  $Q_{ceiling} = 190 \text{ m}^3/\text{h}$  (52.7 litres/second). The contribution of 22 incandescent light fittings at 1.2 Pa would be  $135 \text{ m}^3/\text{h}$  (37.5 litres/second), which is in the right order of magnitude and points towards the downlights as the main conduit of downstairs air into the roof cavity. Additional leakage paths around the roof access hatch or extractor fans are likely to make up the difference.

While the extensive level of mould growth certainly underlines the need for the moisture level in the attic space to be reduced, it is important to point out that there are a number of factors that play an important role in creating and maintaining a healthy building climate. Having established an airtight roof cavity and a ceiling providing easy access for air into the attic, the moisture level of the living spaces is another relevant parameter. To evaluate the indoor climate, temperature and relative humidity were recorded at various points throughout the building over several weeks in 2017. Figure 15 shows the relative humidity (RH) in the roof cavity, kitchen, bathroom and main bedroom for 2 weeks in September.

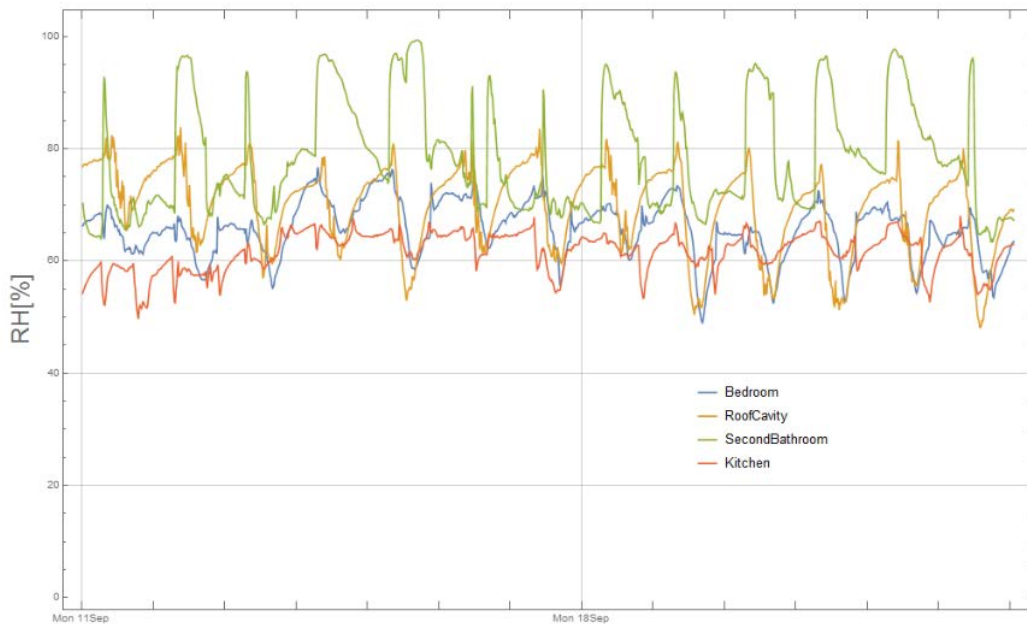


**Figure 15. Relative humidity in the main bedroom, attic space, bathroom and kitchen of the Titirangi dwelling.**

Immediately noticeable are the prolonged periods of time when the relative humidity exceeds 90% in the bathroom. The moisture, probably generated by showers in the morning, is not effectively removed by passive (opening windows) or active (extractor fans) ventilation and remains at a high level for most of the day.

<sup>6</sup> It is assumed here that the airflow across the ceiling is the same in both directions and only dependent on the pressure difference. Pressurising the roof cavity results in an airflow down, whereas in section 2.3.1, it was shown that, under normal conditions, the flow is into the roof cavity.



Looking at the statistical distribution in the form of a box-plot (Figure 16), the following median values for the relative humidity are found: 74% in the bathroom, 75% in the attic, 68% in the bedroom and 63% in the kitchen.

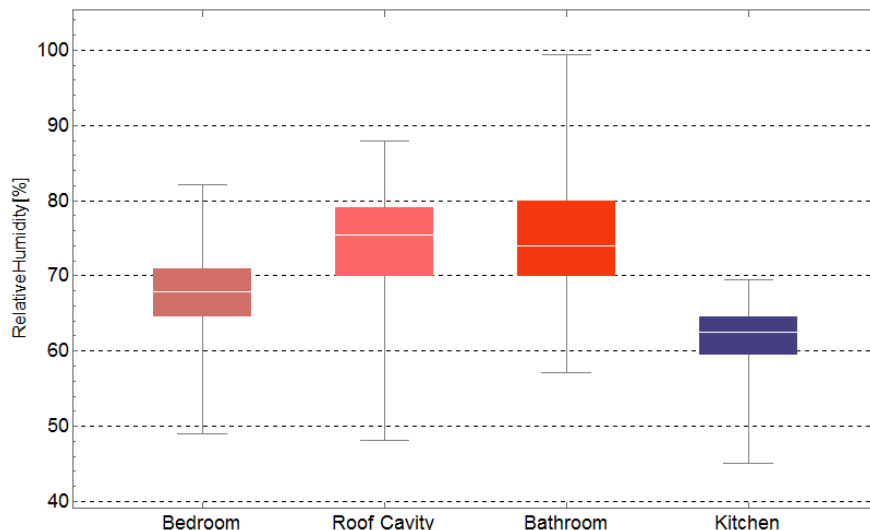


**Figure 16. Statistical distribution of relative humidity for the Titirangi dwelling. The boundaries of the coloured boxes indicate the 25% and 75% quartile, the line represents the median, while the whiskers give the maximum and minimum values.**

Especially the bathroom exhibits high moisture levels. For a quarter of the time, the relative humidity level lies above 80%. If these measurements are representative the occupant behaviour – inadequate ventilation of the living spaces – excessive amounts of moisture will have been transported through the air-leaky ceiling into the attic to accumulate there.

### 3.2.3 Residential building, Papakura, Auckland

This Papakura residential dwelling was completed in early 2017, with signs of mould growth in the roof space shortly thereafter. Like the Titirangi property, the roof construction consists of a south-facing, gable-type roof enclosing a standard roof cavity, adjacent to a north-facing roofline of a skillion-type style. In this case, both the main roof cavity and the much smaller cavity of the skillion part are connected. The total volume was estimated to be 46.2 m<sup>3</sup>. The metal roof cladding is a low-rib type profile with a 9° and 16° slope for the gable-type and skillion part respectively.

The ceiling is lined with plasterboard with square stopping. Downlights are installed in the ceiling throughout the building. However, they are of a recent design with no obvious gaps around the fitting. Mould growth was visible on the roof paper and structural timber, but to a much lesser extent than at the Titirangi property. However, attempts had been made by the occupants previously to clean the surfaces while also using a dehumidifier in the roof space to bring the moisture levels down.

The same measurement procedure – including the dual fan blower door pressurisation tests and indoor climate recording – was performed at this dwelling (Figure 17).



**Figure 17. Measurement set-up with dual fan blower door (left) and ducting into the roof cavity (right).**

The results with and without an airflow across the ceiling are depicted in Figure 18. The roof cavity appeared very airtight, and a pressure of 50 Pa was easily achieved. For the run with fan 1 turned off, instrumental issues prevent any data points being acquired above 25 Pa. At 40 Pascals, the roof envelope alone exhibits an airflow of  $3737 \text{ m}^3/\text{h}$  ( $n50: 4,334 \text{ m}^3/\text{h}$ ), translating to an air exchange rate of 81 ach ( $n50: 94$  ach). Again, using Equation 2, an effective leakage area can be calculated (Table 3). Using the insulated ceiling area and the 1:300 roof ventilation area rule, a benchmark can be established. For this property, the ventilation opening to ceiling area ratio is 45% and even lower than in the Titirangi dwelling. The graphs of the two measurement modes in Figure 18 are closer together than the Titirangi building, pointing towards a more airtight ceiling level and confirming the visual inspection. Extracting the airflow across the ceiling only, by subtracting the two graphs at the reference pressure of 1.2 Pascals, an airflow of  $Q_{\text{ceiling}}(1.2 \text{ Pa}) = 53 \text{ m}^3/\text{h}$  (14.7 litres/second) is estimated.<sup>7</sup> Possible leakage paths have been identified around the roof access hatch, extractor fans and holes for the heat pump services.

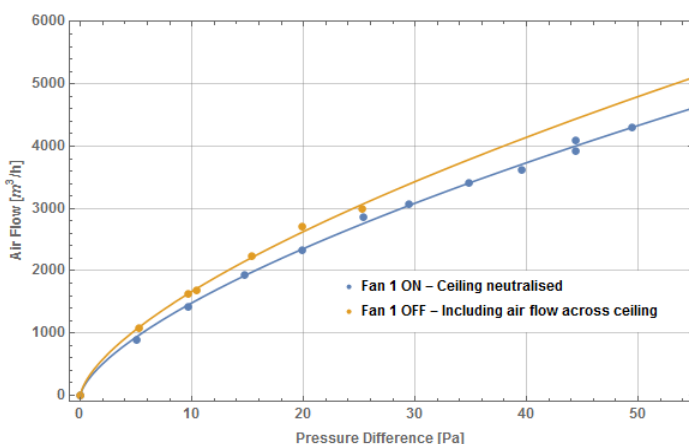


**Figure 18. Airflow results for the Papakura dwelling. The measured data points are fitted using Equation 1.**

The indoor climate was also recorded in September 2017 with data gathered in the main bedroom, roof cavity, bathroom and living room. The statistical parameters for

<sup>7</sup> Given the reduced quality of this dataset, the error is likely increased here.

the relative humidity are given in Figure 19. Noticeable is the much lower humidity levels in the bathroom compared to that of the Titirangi dwelling, which, according to the occupants, is achieved by consistent usage of the extractor fan. The relative humidity in the roof space is very similar to the Titirangi building with a median value of 73%. The distribution of measured values is, however, narrower, mainly due to less extreme temperature variations due to the north-facing aspect of the roof.

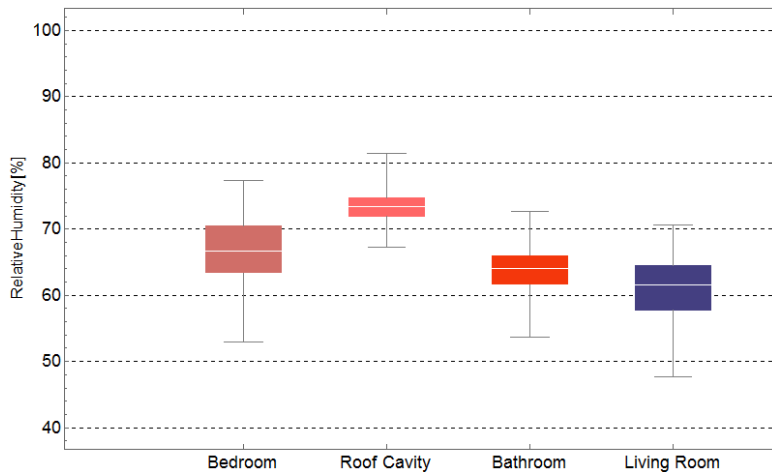


**Figure 19. Statistical distribution of relative humidity for the Papakura dwelling. The boundaries of the coloured boxes indicate the 25% and 75% quartile, the line represents the median, while the whiskers give the maximum and minimum values.**

### 3.2.4 Summary and discussion

Table 3 summarises the results from the dual fan pressurisation measurements performed on the three residential buildings of this study. A reference pressure of 40 Pascals is used to calculate the air exchange rates, since 50 Pa is not always achieved easily in the roof cavity. The effective leakage area of the roof envelope only is calculated using Equation 2. Using the ceiling insulated area, a suggested roof ventilation opening size is calculated based on the 1:300 rule as a benchmark. The measured effective leakage area is compared to this calculated vent opening size, expressed as a percentage.

**Table 3. Ventilation parameters for the three studied dwellings.**

Building	Leakage flow rate @ 40 Pa [m <sup>3</sup> /h]	Roof cavity volume [m <sup>3</sup> ]	Air exchanges/hour @ 40 Pa [ach]	Effective leakage area [cm <sup>2</sup> ]	Ceiling insulated area [m <sup>2</sup> ]	Vent area based on 1:300 rule [cm <sup>2</sup> ]	Measured effective leakage area/suggested area based on 1:300 rule
BRANZ, Wellington	5,930	49.4	120	2,020	90	3,000	67%
Titirangi, Auckland	4,301	58.9	73	1,465	75	2,500	59%
Papakura, Auckland	3,737	46.2	81	1,273	85	2,833	45%

All three buildings characterised in this study fall below the 1:300 ratio. The two buildings in Auckland with mould problems exhibit lower vent openings than the BRANZ test building. While this limited dataset does not allow any general conclusion

on a required roof ventilation rate, it is obvious that the moisture load for the two residential buildings in Auckland is too high. The Titirangi building suffers from a high moisture level in the living spaces due to inadequate ventilation. Especially the bathroom exhibits extremely high moisture levels for prolonged periods of time. With an air-permeable ceiling and a comparatively airtight roof cavity, the moisture level has been allowed to build up to an unhealthy level. The ceiling of the Papakura building is quite airtight. Also, the internal moisture level seems to be at a more acceptable level, with only the bedroom showing relative humidity values in the high 60s. On the other hand, the attic space has the lowest effective leakage area and has less than 50% of the recommended value when using the 1:300 ratio. Construction moisture that has been closed in by this airtight attic space might be the dominant factor.

Additional ventilation to the roof space should help to reduce moisture levels. However, indoor moisture levels, especially in the Titirangi dwelling, need to be improved by ventilation. The ceiling, which currently offers an easy pathway for moisture transport, should also be made more airtight by exchanging the air-leaky downlights.

### 3.2.5 Example: calculation of required roof ventilation

Plagmann (2016) introduced a simple mass-flow balance calculation that can be used to estimate sensible roof ventilation opening sizes. This method is illustrated here, using the experimental data obtained from the Titirangi dwelling.

The calculation is based on the idea that a certain amount of fresh, drier outside air is required to mix with the moist airflow upwards from the living spaces for the attic moisture content to stay below a predefined moisture threshold (Figure 20).

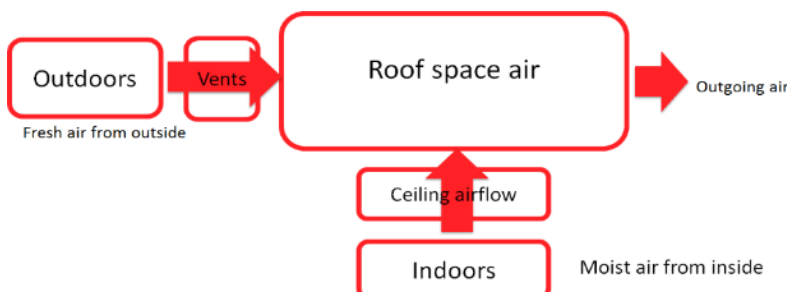


**Figure 20. Sketch of airflows for the mass balance calculation.**

The mass-flow balance is expressed in Equation 3. Here,  $VP$  stands for vapour pressure, which is calculated from temperature and relative humidity.<sup>8</sup> For instance, a climatic condition of  $T=20^\circ\text{C}$  and  $\text{RH}=65\%$  would translate to a vapour pressure of  $VP=1,520 \text{ Pa}$ .

$$\begin{aligned} \text{Vent Flow } & \left[ \frac{\text{m}^3}{\text{h}} \right] \\ & = \frac{\text{Indoor VP [Pa]} - \text{Threshold VP [Pa]}}{\text{Threshold VP [Pa]} - \text{Outdoor VP [Pa]}} \cdot \text{Ceiling Air Flow } \left[ \frac{\text{m}^3}{\text{h}} \right] \quad \text{Eq 3} \end{aligned}$$

The threshold climate is chosen as the maximum allowable relative humidity in the roof cavity, in this case,  $\text{RH}_{\text{threshold}} = 90\%$  at a temperature of  $T_{\text{threshold}} = 12^\circ\text{C}$ . Expressed as a vapour pressure, this yields  $VP_{\text{threshold}} = 1,260 \text{ Pascals}$ . Choosing this particular threshold means that the roof cavity climate should avoid the dew point temperature

<sup>8</sup> See, for instance, the online calculator at <http://go.vaisala.com/humiditycalculator/5.0/>



and thus condensation. The outdoor climate has been chosen as  $T_{\text{outdoor}} = 12^\circ\text{C}$  and  $\text{RH}_{\text{outdoor}} = 80\%$ , translating to a  $\text{VP}_{\text{outdoor}} = 1,120$  Pascals. The indoor climate is obtained from the median relative humidity values of the kitchen/living area, bedroom and bathroom of Figure 16 and a weighting factor considering the different volumes of the rooms. The median temperature is  $T_{\text{indoor}} = 20^\circ\text{C}$  (data not shown) and 66% RH, resulting in a  $\text{VP}_{\text{indoor}} = 1,548$  Pascals to be used in the calculation.

The ceiling airflow in Equation 3 can be taken from our experimental measurements of the ceiling permeability and was estimated to be  $Q_{\text{ceiling}} = 190 \text{ m}^3/\text{h}$  at a pressure difference of 1.2 Pa. Equation 3 now reads:

$$\text{Vent Flow} = \frac{1,548 \text{ Pa} - 1,260 \text{ Pa}}{1,260 \text{ Pa} - 1,120 \text{ Pa}} \cdot 190 \text{ m}^3/\text{h} = 391 \text{ m}^3/\text{h}$$

Thus, assuming this steady-state situation, it would require a flow of 391 m<sup>3</sup>/h (108 l/s) of outside air (12°C/80% RH) into the roof cavity to balance the moist air coming through the ceiling (20°C, 66% RH) in order not to exceed the chosen roof cavity climate threshold of 12°C and 90% RH.

The second step now is to determine what passive vent elements will yield this required airflow. Achieving this flow will depend on the prevailing wind conditions, the vent position and its airflow characteristics. In the absence of reliable data, the wind conditions for the specific site need to be estimated. Ventilation is driven by wind action, and consequently, it is the lower wind speed conditions that increase the risk of inadequate ventilation. The relationship between wind speed and induced pressure at a given location of the dwelling is

$$p = 0.6 \cdot C_p \cdot V^2 \quad \text{Eq 4}$$

with  $V$  being wind speed [m/s],  $C_p$  the building pressure coefficient and  $p$  the induced pressure [Pa]. For a location at the eaves,  $C_p$  is assumed to be 0.8. The wind speed is taken as 1.5 m/s for this calculation,<sup>9</sup> resulting in a pressure of 1.1 Pa at the eaves.

A variety of different vent elements has been characterised by BRANZ, and the results will be published elsewhere. Here, a simple rectangular metal mesh of 12 mm width is used, which, at 1.1 Pa, will yield an airflow of 12 l/s/m. Thus, to achieve the required vent flow of 391 m<sup>3</sup>/h (108 l/s), 9 metres of this mesh needs to be installed on either side of the roof cavity. The net free opening of this vent element is then 2·0.11 m<sup>2</sup> (2,200 cm<sup>2</sup>).

The calculated value for the recommended ventilation opening size (2,200 cm<sup>2</sup>) is larger than the effective leakage area that has been measured for this dwelling (1,465 cm<sup>2</sup>) and lies closer the benchmark value derived from the 1:300 rule (2,500 cm<sup>2</sup>). It is necessary to point out that the calculation relies on a number of assumptions and estimates and can only give an order of magnitude. However, in this case, it does suggest that the roof cavity is too airtight, which is confirmed by the problematic mould growth. The maximum relative humidity in the attic space (Figure 16) did not actually exceed 88% for this measurement period. The reason for this might be that the outdoor climate conditions were more favourable than the worst-case scenario of the above calculation.

---

<sup>9</sup> The lower wind speed quantile for Auckland in winter is approximately 2 m/s. The Titirangi dwelling, however, is located in a valley and likely to experience less wind pressure.



## 4. Conclusions and outlook

We have introduced and trialled a measurement procedure that allows us to estimate the airtightness of residential roof spaces. By using a dual fan approach, it is possible to distinguish between the leakage through the roof envelope and the air permeability of the ceiling. This is important in order to derive an effective leakage area for the roof envelope only, which can then be used to benchmark buildings with and without roof space moisture problems. It is also possible to quantitatively compare our buildings to overseas standards with prescribed roof ventilation requirements (for instance the 1:300 rule). Measurements on a standard residential building can be completed in a matter of 1–2 hours.

Knowledge of the air permeability of the ceiling is important since the living space is often a source of moisture that can end up in the attic space. Real-world data for ceilings derived from our dual fan measurements can be compared to data generated at our test facility at BRANZ. Here, we have started to characterise common ceiling types as well as ceiling penetrations such as light fittings. The datasets are given in a tabular form and can be used in numerical simulations.

The recorded climate data from mould-affected roof cavities will be used to verify WUFI Bio,<sup>10</sup> which is a recent addition to the popular WUFI moisture transport simulation programme. The WUFI Bio add-on aims to predict mould growth from climatic and material properties and would be a valuable tool to specify roof ventilation requirements.

---

<sup>10</sup> <https://wufi.de/en/2017/03/31/wufi-bio/>

## References

- ASHRAE. (2009). *ASHRAE handbook – fundamentals*. Atlanta, USA: American Society of Heating, Refrigerating and Air-Conditioning Engineers.
- BRANZ. (2014). *Aggravated thermal bridging research*. Bulletin BU572. Judgeford, New Zealand: BRANZ Ltd.
- BRANZ. (2017). *Preventing moisture problems in timber-framed skillion roofs*. Bulletin BU610. Judgeford, New Zealand: BRANZ Ltd.
- Essah, E. (2012). Domestic cold pitched roofs in the UK – effect of using different roof insulation materials. *International Journal of Ventilation*, 11(3), 281–296.
- Liddament, M. (1986). *Air infiltration calculation techniques: An applications guide*. Coventry, UK: Air Infiltration and Ventilation Centre.
- Lstiburek, J. (2004). *Roof design*. Research report RR-0404. Westford, MA: Building Science Corporation.
- McNeil, S., Quaglia, L., Bassett, M., Overton, G. & Plagmann, M. (2012). A survey of airtightness and ventilation rates in post 1994 homes. *Proceedings of the 33rd AIJC Conference "Optimising Ventilative Cooling and Airtightness for [Nearly] Zero-Energy Buildings, IAQ and Comfort"*, Copenhagen, Denmark, 10–11 October.
- Overton, G. (2018). Flat-out testing! *Build*, 165, 52–53.
- Plagmann, M. (2016). Roof ventilation. *Build*, 157, 57–58.
- Roppel, P., Norris, N. & Lawton, M. (2013). Highly insulated, ventilated, wood-framed attics in cool marine climates. *Proceedings of the Thermal Performance of the Exterior Envelopes of Whole Buildings XII International Conference*, Clearwater, Florida, 1–5 December.
- Rupp, S. (2018). Cold roofs? Warm roofs? *Build*, 164, 78–79.
- Rupp, S. & Plagmann, M. (2016). *Numerical simulation of ventilation in roof cavities*. BRANZ Study Report SR343. Judgeford, New Zealand: BRANZ Ltd.
- Sherman, M. H. (1990). Tracer-gas techniques for measuring ventilation in a single zone. *Building and Environment*, 25(4), 365–374.

## Appendix A: Fan calibration

The airflow rate through the fan for its different fan speeds is obtained by measuring the pressure difference across the nacelle. This fan pressure is calibrated against an airflow rate. The measured fan pressure must be high enough to get a good signal-to-noise ratio, which can be difficult to achieve for an airtight dwelling with a low airflow rate into the building. To increase the fan pressure for a given airflow rate, restrictor plates can be mounted to the fan. The possible configurations are depicted in Figure 21.

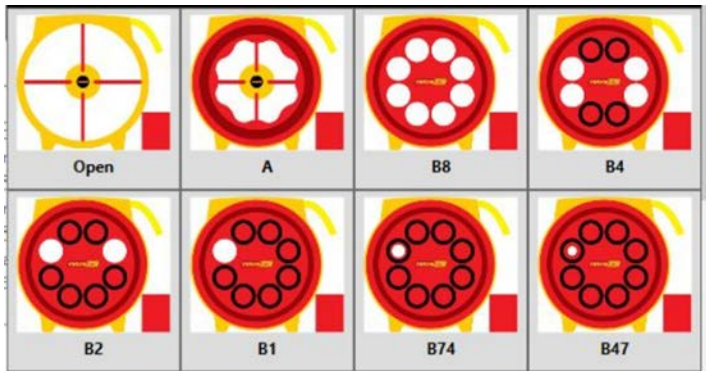


**Figure 21. Restrictor plate configurations for the Retrotec fans.**

The 6000-series fan was used to pressurise the BRANZ ventilation house to 50 Pa. In a first reference test, the fan was used without any ducting to give the true airflow. Ducting was then gradually attached in different configurations and the test repeated. It was found that, when using the open configuration in combination with ducting attached to the fan, the measured airflow rate was overestimated.

**Table 4. Ducting error results.**

Test configuration	Airflow rate	Error
Test 1: Reference, no ducting	1860 l/s	-
Test 2: Open fan configuration, 5 m Retrotec ducting straight out from the fan	2000 l/s	+7.5%
Test 3: Open fan configuration, 5 m orange flexi-ducting straight out from the fan but unstretched	2140 l/s	+15%
Test 4: Open fan configuration, 5 m orange flexi-ducting, with 90° bent and stretched out	2290 l/s	+23%

Fan pressure measurement errors will be much smaller when using the A or B8 restrictor plates instead of it being open. Only these configurations were used for testing.